Interpenetrated metal–organic frameworks and their uptake of CO

ARTICLE *in* JOURNAL OF MATERIALS CHEMISTRY · JANUARY 2012

Impact Factor: 7.44

6 AUTHORS, INCLUDING:

Ocean Cheung

Uppsala University

17 PUBLICATIONS **134** CITATIONS

SEE PROFILE

Xiaodong Zou

Stockholm University

265 PUBLICATIONS **3,750** CITATIONS

SEE PROFILE

Journal of Materials Chemistry

Cite this: *J. Mater. Chem.*, 2012, **22**, 10345

www.rsc.org/materials

PAPER

Interpenetrated metal–organic frameworks and their uptake of CO_2 at relatively low pressures†

Qingxia Yao, Jie Su, Ocean Cheung, Qingling Liu, Niklas Hedin* and Xiaodong Zou*

Received 16th November 2011, Accepted 8th February 2012
DOI: 10.1039/c2jm15933c

Adsorption-driven separation of CO_2 from flue gas has the potential to cut the cost for carbon capture and storage. Among the porous physisorbents, metal–organic frameworks (MOFs) are a class of promising candidates for gas separation and storage owing to their extraordinarily high specific surface areas and pore volumes, and predesigned pore structures. Here, we report three interpenetrated MOFs composed of Zn_4O clusters and rigid dicarboxylate anions, namely SUMOF-*n* (SU = Stockholm University; $n = 2, 3, 4$). All the interpenetrated MOFs possess small pores of two different types and high pore volumes. SUMOF-2 had a structure similar to interpenetrated MOF-5, but with an extra-framework cation present in one of the two types of pores. SUMOF-3 was an interpenetrated version of IRMOF-8 while SUMOF-4 crystallized with mixed linkers, biphenyl-4,4′-dicarboxylic acid and benzene-1,4-dicarboxylic acid. Among the three SUMOFs, SUMOF-4 had the largest specific surface area (1612 $m^2\ g^{-1}$) and pore volume. Single component adsorption of CO_2 and N_2 was determined at 273 K. We showed that the interpenetrated SUMOF-2 adsorbed more CO_2 than non-interpenetrated MOF-5 under 273 K and 1 bar. This may be explained by the increased electric field gradients due to the interpenetration in the MOF. The uptake of CO_2 for SUMOF-2 and SUMOF-4 was significant at somewhat higher pressure. Their CO_2 isotherms were close to linear, which could be beneficial for separation of CO_2 *via* pressure swing adsorption from biogas or natural gas. On the other hand, SUMOF-3 adsorbed most CO_2 at pressures relevant for CO_2 capture from flue gas.

Introduction

Adsorption-driven separation of CO_2 from N_2-rich flue gas mixtures is highly relevant for the economics of carbon capture and storage (CCS). Today, CO_2 is typically captured by liquid amines, but adsorption-driven processes could potentially cut the cost for such capture significantly.[1] Choi *et al.*,[2] Hedin *et al.*,[3] and D'Alessandro *et al.*[4] have reviewed adsorbents for CO_2 capture in general. Rapid uptake, high capacity, high selectivity for CO_2, appropriate heat and mass transfer characteristics and mechanical properties are all important for adsorbents for CO_2 capture. The partial pressure of CO_2 in flue gas is about 0.1 bar at a total pressure of 1–1.5 bar. A 1000 MW coal-fired power plant produces ~1000 ton-CO_2 per h, and it appears to be almost inconceivable to compress flue gas. Hence, a physisorbent for post-combustion capture of CO_2 should have small pores. This is because the electric field gradients are greater in small pores and these interact with the significant quadrupole moment of CO_2, causing a larger tendency to adsorption than in large pores. In addition, CO_2 interacts more frequently with multiple walls/chains in small pores than in large pores.

Microporous metal–organic frameworks (MOFs) composed of inorganic and organic building units are promising porous materials with many applications in gas storage, separation, and catalysis.[5] Bae and Snurr recently reviewed how MOFs and related adsorbents for CO_2 separation and capture could be rapidly evaluated, which is relevant due to the very rich chemistry of MOFs.[6] For separation and purification of small gas molecules such as CO_2, N_2, H_2, and CH_4, MOFs with interpenetrated structures have great potential, since their pore apertures can be tuned to the size of the gas molecules.[4,6] For example, interpenetrated MOFs have shown significant uptake of H_2.[7,8] Chen *et al.* showed that a doubly interpenetrated Cu-MOF[9] and a triply interpenetrated Cu-MOF[10] had significant uptake of CO_2 at 195 K and a very low uptake of N_2 at 77 K. Cheon and Suh studied a four-fold interpenetrated Ni-MOF with cyclam and methanetetrabenzoate ligands had significant uptake of CO_2 and a negligible uptake of N_2.[11] Bastin *et al.* showed the first example of separation and removal of CO_2 from binary CO_2/N_2 and CO_2/CH_4 as well as ternary $CO_2/N_2/CH_4$ mixtures at fixed bed using an interpenetrated MOF, MOF-508b.[12]

Here, we present the syntheses and structures of three two-fold interpenetrated MOFs based on Zn_4O clusters and rigid dicarboxylic acids. All the three MOFs have narrow pores and are thermally stable up to at least 400 °C. We focus on their capacity and the

Berzelii Centre EXSELENT on Porous Materials and Department of Materials and Environmental Chemistry, Stockholm University, Stockholm, SE-106 91, Sweden. E-mail: xzou@mmk.su.se; niklas.hedin@mmk.su.se; Fax: +46 8 15 21 87; Tel: +46 8 16 23 89

† Electronic supplementary information (ESI) available: Crystal data and details of structure refinement, thermogravimetric analysis, stability of activated SUMOFs. CCDC reference numbers 853630–853632. For ESI and crystallographic data in CIF or other electronic format see DOI: 10.1039/c2jm15933c

apparent selectivity for CO_2 sorption at low pressure. Their pressure dependencies for the uptake of CO_2 and of N_2 were investigated and discussed in the context of capture of CO_2 from point sources.

Experimental

Synthesis

SUMOF-2, SUMOF-3, and SUMOF-4 were synthesized under solvothermal conditions from $Zn(NO_3)_2 \cdot 6H_2O$ and corresponding rigid dicarboxylic acids in dimethylformamide (DMF) (Scheme 1). Colorless crystals large enough for single crystal X-ray diffraction analysis were obtained.

SUMOF-2, which is related to an interpenetrated analogue of MOF-5, was synthesized by first dissolving $Zn(NO_3)_2 \cdot 6H_2O$ (600 mg, 2 mmol; Sigma-Aldrich, CAS number 10196-18-6) and benzene-1,4-dicarboxylic acid (H_2BDC, 170 mg, 1 mmol; Aldrich, CAS number 100-21-0) in 20 mL of DMF (VWR, CAS number 68-12-2). The solution was solvothermally treated in a 30 mL Teflon-lined autoclave at 120 °C for 24 h, under static conditions. Colorless cubic crystals formed (yield ≈ 300 mg), which were filtered, washed with DMF, and dried at room temperature. The chemical formula of activated SUMOF-2 is $[Zn_4O(BDC)_3] \cdot (ZnO)_{0.125}$ as deduced from the structure refinement and the elemental analysis (wt%): exp: C 36.61, H 1.742, N 0.034; calcd: C 36.96, H 1.529, N 0.

SUMOF-3, which is an interpenetrated analogue of IRMOF-8, was synthesized by first dissolving $Zn(NO_3)_2 \cdot 6H_2O$ (117 mg, 0.39 mmol) and 2,6-naphthalenedicarboxylic acid (H_2NDC, 54.8 mg, 0.25 mmol; Aldrich, CAS number 1141-38-4) in 5 mL of DMF in a 20 mL glass vial. The solution was solvothermally treated at 130 °C for 28 h, under static conditions. Yellow crystals formed (yield ≈ 70 mg). The crystals were filtered, washed with DMF, and dried at room temperature. The chemical formula of activated SUMOF-3 is $[Zn_4O(NDC)_3]$, as deduced from the structure refinement and the elemental analysis (wt%): exp: C 46.36, H 2.240, N 0.051; calcd: C 46.99, H 1.970, N 0.

SUMOF-4 was synthesized by first dissolving $Zn(NO_3)_2 \cdot 6H_2O$ (228 mg, 0.76 mmol), benzene-1,4-dicarboxylic acid (H_2BDC, 83 mg, 0.50 mmol), and biphenyl-4,4′-dicarboxylic acid (H_2BPDC, 61 mg, 0.25 mmol; Aldrich, CAS number 787-70-2) in 10 mL of DMF in a 20 mL glass vial. The solution was solvothermally treated at 130 °C for 4 h, under static conditions. Colorless prism crystals formed (yield ≈ 120 mg). The crystals were filtered, washed with DMF, and dried at room temperature. The chemical formula of activated SUMOF-4 is $[Zn_4O(BDC)_2(BPDC)(H_2O)]$, as deduced from the structure refinement and the elemental analysis (wt%): exp: C 41.24, H 2.205, N 0.029; calcd: C 41.66, H 2.083, N 0. Elemental analysis indicates that coordinated water molecules were retained after activation at 200 °C.

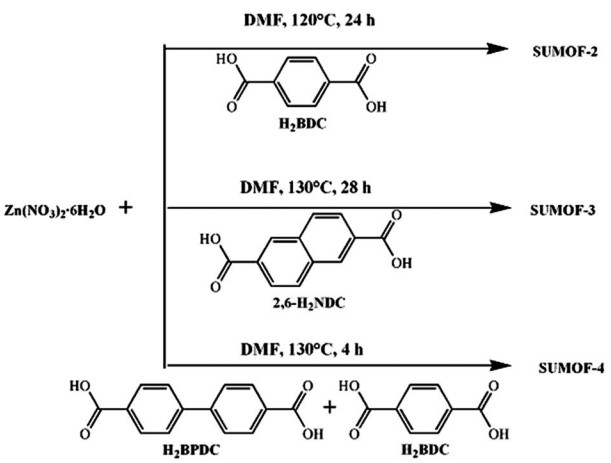

Scheme 1 Synthesis of the SUMOFs.

Powder X-ray diffraction (PXRD)

PXRD data were collected on a PANalytical X'Pert Pro diffractometer using Cu $K_{\alpha 1}$ ($\lambda = 1.5406$ Å) radiation, recorded on a Pixel detector at a speed of 2° (2θ) min^{-1}. Samples were dispersed uniformly on plates of silicon with a zero-background by using isopropanol.

Structure determination by single crystal X-ray diffraction

Single crystal X-ray diffraction data were recorded at room temperature on an Oxford Diffraction Xcalibur 3 diffractometer, with Mo K_α radiation ($\lambda = 0.71073$ Å). Data reduction was performed using the CrysAlisPro program and multi-scan adsorption correction was applied. Structures were solved by direct methods. Non-hydrogen atoms were located directly from difference Fourier maps. Framework hydrogen atoms were placed geometrically and constrained in the riding model to the parent atoms. Final structure refinements were performed with the SHELX program[13a] by minimizing the sum of the squared deviations of F^2 using a full-matrix technique. High symmetry and large pore sizes of the MOFs, as well as disorders of the guest molecules (DMF and H_2O) in the pores, precluded location of these guest molecules. The PLATON/SQUEEZE program was used to remove scattering contribution from disordered guest molecules and to produce solvent-free diffraction intensities, which were used in the final structure refinement.[13b] Due to large fractional pore volumes, intensities and resolution of the diffraction data were rather poor as indicated by the low I/σ, high R_{int} and low 2θ angles. These effects also resulted in relatively high R values in the final refinements. A summary of crystal data and structure refinement of the SUMOFs is given in footnote‡ and more details are presented in Table S1†.

‡ *Crystal data for SUMOF-2*: $M_w = 794.24$, trigonal, space group $R\bar{3}m$, $a = 18.4010(10)$ Å, $c = 44.057(3)$ Å, $V = 12\,918.9(14)$ Å^3, $Z = 12$, $D_{calc} = 1.225$ g cm^{-3}, $F(000) = 4704$, μ(Mo-K$_\alpha$) = 2.314 mm^{-1}, crystal size 0.30 × 0.30 × 0.25 mm, $T = 293(2)$ K, θ range = 4.13–26.37°, 29 350 reflections measured, 3211 independent ($R_{int} = 0.1114$), $R1 = 0.0890$, w$R2 = 0.2153$ for 2326 reflections with $I > 2\sigma(I)$, and $R1 = 0.1143$, w$R2 = 0.2308$ for all data, GOF = 1.098. CCDC 853630.
Crystal data for SUMOF-3: $M_w = 1995.32$, triclinic, space group $P\bar{1}$, $a = 18.6086(8)$ Å, $b = 20.2422(7)$ Å, $c = 20.8135(7)$ Å, $\alpha = 70.421(3)°$, $\beta = 68.955(3)°$, $\gamma = 68.031(4)°$, $V = 6600.7(4)$ Å^3, $Z = 2$, $D_{calc} = 1.004$ g cm^{-3}, $F(000) = 2001$, μ(Mo-K$_\alpha$) = 1.479 mm^{-1}, crystal size 0.20 × 0.15 × 0.15 mm, $T = 293(2)$ K, θ range =4.14–26.37°, 45 520 reflections measured, 26 227 independent ($R_{int} = 0.0490$), $R1 = 0.0590$, w$R2 = 0.1616$ for 15 115 reflections with $I > 2\sigma(I)$, and $R1 = 0.0916$, w$R2 = 0.1745$ for all data, GOF = 1.002. CCDC 853631.
Crystal data for SUMOF-4: $M_w = 936.01$, orthorhombic, space group *Pnnm*, $a = 18.3770(6)$ Å, $b = 17.3043(4)$ Å, $c = 17.9565(5)$ Å, $V = 5710.2(3)$ Å^3, $Z = 4$, $D_{calc} = 1.089$ g cm^{-3}, $F(000) = 1876$, μ(Mo-K$_\alpha$) = 1.705 mm^{-1}, crystal size 0.25 × 0.20 × 0.20 mm, $T = 293(2)$ K, θ range = 4.20–26.37°, 19 462 reflections measured, 5966 independent ($R_{int} = 0.0419$), $R1 = 0.0545$, w$R2 = 0.1828$ for 4341 reflections with $I > 2\sigma(I)$, and $R1 = 0.0738$, w$R2 = 0.1937$ for all data, GOF = 1.086. CCDC 853632.

Thermogravimetric analysis (TGA)

TGA was performed on a Perkin Elmer TGA 7 analyzer to study the thermal stability and the quantity of solvent guest molecules present in the SUMOFs. The SUMOFs were heated from 30 °C to 700 °C at a heating rate of 10 °C min^{-1} in a platinum holder under a continuous flow of dry air.

N_2 adsorption at 77 K

N_2 adsorption–desorption isotherms were recorded at 77 K on a Micromeritics ASAP2020 analyzer. The SUMOFs were degassed under N_2 flow at 473 K for 3 h and subsequently under dynamic vacuum at 473 K for 6 h. Specific surface areas were calculated from the data in the adsorption branch at $p/p_0 = 0.05$–0.15. Total pore volumes were calculated from the uptake at p/p_0 of 0.985.

Adsorption of CO_2 and N_2 at 273 K

Adsorption and desorption isotherms of CO_2 and N_2 were recorded at 273 K for degassed SUMOFs at pressures of 0.0004–1 atm on a Micromeritics ASAP2020 device. For each SUMOF, about 200 mg of the sample was degassed using the same procedure as described above. The temperature was controlled during the measurements.

Results and discussion

Synthesis and characterization of interpenetrated SUMOFs

High concentrations of reactants, high temperatures or long reaction time usually result in interpenetrated MOFs. In our case, SUMOF-2 and 3 can be regarded as interpenetrated analogues of MOF-5 and IRMOF-8, respectively.[14] SUMOF-2 was synthesized under similar conditions as those described by Hafizovic *et al.*,[15] except that a longer reaction time was used. Materials of the MOF-5 type have been reported to be highly sensitive to the preparation method.[15,16] It is worthy to note that for our synthesis, the zinc source, $Zn(NO_3)_2 \cdot 6H_2O$, was kept intact to avoid water from air being adsorbed onto it. Otherwise, one could observe multiple impurities in the product, including a large quantity of ZnO spherical particles, as usually observed in synthesis of MOF-5.[17] SUMOF-3, a two-fold interpenetrated analogue of IRMOF-8, was synthesized with a higher concentration of H_2NDC at higher temperature, comparing with those for the synthesis of IRMOF-8.[18] To our knowledge, synthesis of pure interpenetrated IRMOF-8 has not yet been reported, although it has been proposed.[18,19] SUMOF-4 was synthesized with mixed linkers, H_2BPDC and H_2BDC. For all three SUMOFs, phase purity was confirmed by both PXRD and TGA analysis (see ESI, Fig. S1†). The chemical formula of the activated SUMOFs as deduced from the structure refinement is $[Zn_4O(BDC)_3] \cdot (ZnO)_{0.125}$ for SUMOF-2, $[Zn_4O(NDC)_3]$ for SUMOF-3, and $[Zn_4O(BDC)_2(BPDC)(H_2O)]$ for SUMOF-4, which match those from the TGA analysis (see ESI, Fig. S1†) and elemental analysis.

Structures of SUMOF-2, SUMOF-3 and SUMOF-4

The structures of the three SUMOFs are all composed of Zn_4O clusters combined with different linkers, and exhibit the **pcu** net topology with two-fold interpenetration (Fig. 1). Each Zn_4O cluster is coordinated to six dicarboxylate anions, linking the coordination frameworks in three dimensions. Similar Zn_4O clusters are present in many MOFs.[5a,b,f,h,j,14]

SUMOF-2 is a doubly interpenetrating analogue of MOF-5. The single network of SUMOF-2 is built from Zn_4O clusters linked by BDC anions (Fig. 1a). SUMOF-2 has two different types of cavities with the free diameter of 5.9 Å and 7.7 Å, respectively (Fig. 1b). Similar interpenetrated MOF-5 structures were previously reported,[16a,f] with water molecules occupied in the small cavities. The structure refinement of SUMOF-2 showed a very high electron density in the center of the small cavities, which was almost twice the density of a fully occupied oxygen atom. EDS (Energy Dispersive X-Ray Spectroscopy) and ICP-OES (Inductively Coupled Plasma Optical Emission Spectroscopy) revealed zinc to be the only element present in the sample with an atomic number higher than oxygen's. Therefore, the high electron density in the cavities was assigned to Zn^{2+} cations. The final structure refinement gave an occupancy of 0.5 for Zn^{2+}. The

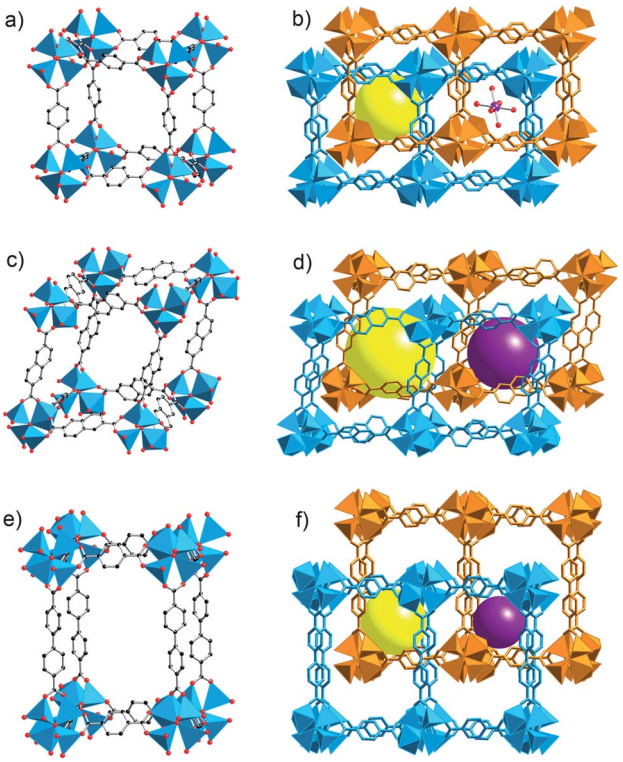

Fig. 1 Non-interpenetrated models (left column) and crystal structures of the doubly interpenetrated frameworks. (a) One of the two interpenetrated frameworks of SUMOF-2, known as MOF-5. (b) The framework of SUMOF-2 showing one pore with the size of 7.7 Å and Zn^{2+} cation in the small cage. (c) One of the two interpenetrated frameworks of SUMOF-3, known as IRMOF-8. (d) The framework of SUMOF-3 showing two pores with the size of 9.5 Å (yellow) and 6.6 Å (purple). (e) One of the two interpenetrated frameworks of SUMOF-4. (f) The framework of SUMOF-3 showing two pores with the size of 7.9 Å (yellow) and 6.0 Å (purple).

coordination sphere of extra-framework Zn^{2+} probably consists of partially occupied oxygen atoms forming $Zn(OH)_6$ species. Thus, the small cavities are partially blocked by Zn^{2+}. This kind of pore filling effects by the Zn-species also can be observed in MOF-5.[15] The total solvent-accessible volume of the desolvated framework, after removal of guest solvates and coordinated water molecules, was estimated to be 44.2% using the PLATON/VOID routine. The charge of these extra-framework cations is most probably balanced by hydroxyl groups connected to the Zn_4O clusters.

The powder XRD pattern of as-synthesized SUMOF-2 matched well with the simulated one, based on the structure determined by single crystal X-ray diffraction, as shown in Fig. 2a. Two intense peaks at 9.6° and 9.8° were detected in the pattern of as-synthesized SUMOF-2, whereas non-interpenetrated MOF-5 only showed one peak, at 9.7°. The splitting of the peaks disappeared after SUMOF-2 was heated for 6 hours at 200 °C in dynamic vacuum. This disappearance is probably related to symmetry changes associated with the removal of guest molecules. Although the peak positions in the PXRD patterns were almost identical for SUMOF-2 and MOF-5, peak intensities differed significantly for the two structures. The intensity distribution in the experimental PXRD patterns of SUMOF-2 was similar to a simulated one based on the structure of SUMOF-2, which confirms that SUMOF-2 is a two-fold interpenetrated MOF-5 structure.

SUMOF-3 is built up by Zn_4O clusters and the NDC linkers and can be regarded as a two-fold interpenetrated analogue of IRMOF-8 (Fig. 1c and d). Three of the Zn atoms in the Zn_4O cluster are tetrahedrally coordinated to form ZnO_4 and one is octahedrally coordinated to form ZnO_6. Each Zn_4O cluster is connected to six NDC linkers and two water or DMF molecules. SUMOF-3 has two types of cavities, with free diameters of about 6.6 Å and 9.5 Å, respectively. The total solvent-accessible volume of the desolvated framework, after removal of guest solvates and coordinated water molecules, was calculated to be 58.3%. The octahedral coordination of one of the Zn atoms and the π–π interaction between the two interpenetrating frameworks led to significant distortions of the unit cell, from ideal cubic to triclinic.

Rowsell and Siberio-Pérez *et al.* suggested that IRMOF-8 has a tendency to form interpenetrated versions.[19] However, no pure interpenetrated analogue of IRMOF-8 was reported. The simulated PXRD patterns of IRMOF-8 with a single network and SUMOF-3 with a doubly interpenetrated framework differ significantly, as shown in Fig. 2b. The PXRD pattern of the as-synthesized SUMOF-3 is similar to the simulated PXRD patterns of SUMOF-3, indicating that the bulk sample contains interpenetrated framework SUMOF-3. The PXRD pattern of activated SUMOF-3, after removal of the guest molecules, changed significantly as compared to that of the as-synthesized SUMOF-3, indicating that the framework of SUMOF-3 is rather flexible and changes from the original framework structure after activation.

SUMOF-4 was synthesized using mixed linkers and crystallized in the orthorhombic space group *Pnnm*. The asymmetric unit of SUMOF-4 contains one Zn_4O cluster, one BDC linker, one BPDC linker, one coordinated water and one DMF molecule. Similar to those in SUMOF-3, three of the Zn atoms in the Zn_4O cluster are tetrahedrally coordinated to form ZnO_4 and one is octahedrally coordinated to form ZnO_6. Each Zn_4O cluster is connected to four BDC linkers to form a two-dimensional square network, which is further linked by BPDC anions to form a three-dimensional framework, as shown in Fig. 1e and f. DMF or water molecules are coordinated to the ZnO_6 octahedron as terminal groups. The framework of SUMOF-4 also adopts a two-fold interpenetration as SUMOF-2 and -3. Because of the longer BPDC linkers, the void space in

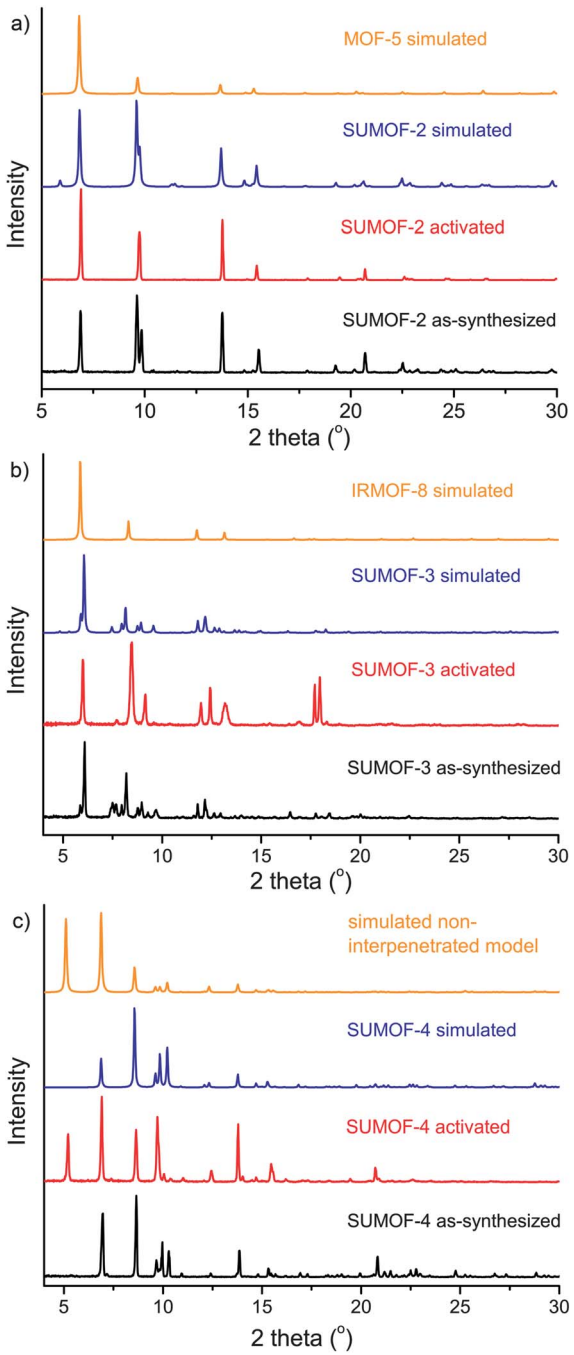

Fig. 2 Powder X-ray diffraction patterns for SUMOF-2 (a), SUMOF-3 (b) and SUMOF-4 (c): as-synthesized (black line), activated (red line), simulated (blue line), and simulation of non-interpenetrated frameworks (orange line).

SUMOF-4 (54.4% as calculated by PLATON) is larger than that in SUMOF-2, which is filled by DMF and water molecules. In SUMOF-4, the cavities have free diameters of 6.0 Å and 7.9 Å, respectively. The PXRD pattern of the as-synthesized SUMOF-4 was very similar to that simulated based on the refined structure of SUMOF-4, implying that there is no impurity in the powder sample. The PXRD pattern of activated SUMOF-4 showed an extra peak at a low 2θ angle (5.1°), which corresponds to the 010 reflection of SUMOF-4. The 010 reflection was absent due to the *Pnnm* symmetry in the as-synthesized SUMOF-4, but present in the activated sample. This difference indicates that when the guest species are removed, symmetry of SUMOF-4 changes. The simulated PXRD pattern of a single SUMOF-4 network is also shown in Fig. 2c, which differs significantly from the as-synthesized SUMOF-4, confirming that the sample was pure. The single SUMOF-4 network also has a different symmetry than the interpenetrated SUMOF-4.

Thermogravimetric analysis (TGA)

TGA curves for the interpenetrated MOFs are given in Fig. S1†. SUMOF-2, 3 and 4 lost all their solvents at 250, 200 and 200 °C, and started to decompose at 480, 420 and 420 °C, respectively.

Adsorption of N_2 at 77 K

TGA analysis (Fig. S1†) shows that all occluded guest solvents in SUMOFs were removed from the pores at 473 K. The N_2 adsorption and desorption isotherms at 77 K for SUMOF-2, SUMOF-3 and SUMOF-4 are presented in Fig. 3. SUMOF-4 showed a higher uptake of N_2 than SUMOF-2 and SUMOF-3 at relative pressures (p/p_0) of $N_2 > 10^{-4}$. SUMOF-4 has a larger specific pore volume than SUMOF-2 and SUMOF-3, see Table 1. Obviously, this finding is not consistent with the calculated voids based on the crystal structures. This difference could possibly be related to a relative shift of single networks with respective to each other after activation, leading to changes of the void. The area was the largest for SUMOF-4 (1612 $m^2\ g^{-1}$), which can be rationalized by the extended and thin biphenylic groups in the structure. The BET model failed to represent data well and it is not ideal to assume multilayer adsorption in the very narrow pores of these SUMOFs. Hence, the specific surface areas were calculated using the Langmuir model, which represented the data very well. For relative N_2 pressure (p/p_0) of 10^{-5} to 10^{-4}, SUMOF-2 had a significantly higher uptake than did SUMOF-3 and SUMOF-4. This difference is related either to the smaller window of SUMOF-2 compared with the others, or most possibly to the presence of the extra framework cations in SUMOF-2.

Table 1 Specific pore volumes and surface areas for the SUMOFs

Material name	Langmuir surface area/$m^2\ g^{-1}$	Pore volume/$cm^3\ g^{-1}$
SUMOF-2	1167	0.421
SUMOF-3	1163	0.440
SUMOF-4	1612	0.580

Adsorption of CO_2 and N_2 at 273 K

The adsorption isotherms for CO_2 and N_2 were determined at 273 K for SUMOF-2, SUMOF-3 and SUMOF-4 and are presented in Fig. 4 and 5. All the SUMOFs showed higher uptake for CO_2 than for N_2. At CO_2 pressures of 100 kPa, the uptake of CO_2 for SUMOF-2, SUMOF-3 and SUMOF-4 at 273 K was 4.26, 3.44, and 3.60 mmol g^{-1}, while the uptake of N_2 was 0.27, 0.19, and 0.17 mmol g^{-1} respectively. The uptake of CO_2 for SUMOF-2 compared well with that of Zn-aminotriazolato-oxalate (4.3 mmol g^{-1} at 273 K).[20] It is interesting to note that the uptake of CO_2 for SUMOF-2 was remarkably higher than that of non-interpenetrated MOF-5 (1.50 mmol g^{-1} or 66.1 mg g^{-1} at 100 kPa and 273 K).[21] This difference can be ascribed to the increased electric field gradients due to the interpenetration in SUMOF-2.

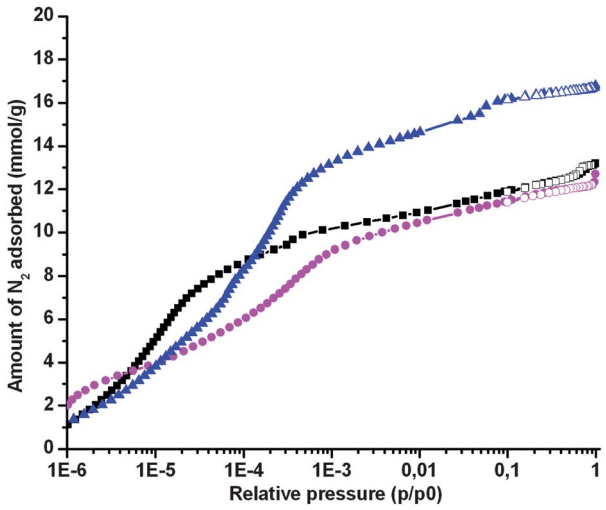

Fig. 3 The N_2 uptake at 77 K *versus* pressure for the SUMOFs. Black squares (■) for SUMOF-2, magenta circles (●) for SUMOF-3, and blue triangles (▲) for SUMOF-4. Adsorption is denoted by filled symbols and desorption by empty symbols.

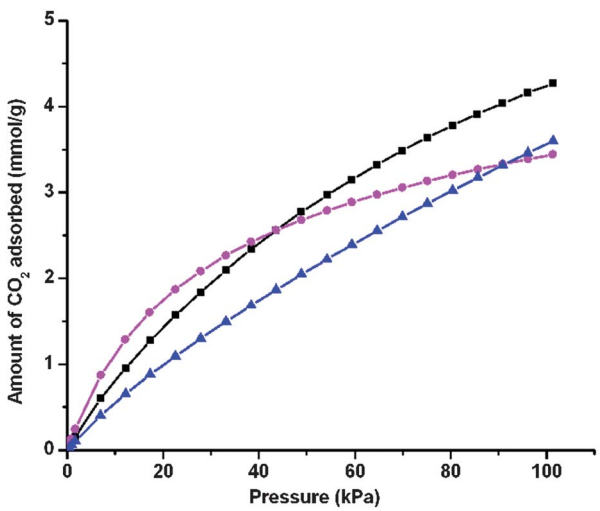

Fig. 4 Adsorption of CO_2 at 273 K *versus* pressure for interpenetrated metal–organic frameworks (MOFs); black squares (■) for SUMOF-2, magenta circles (●) for SUMOF-3, and blue triangles (▲) for SUMOF-4.

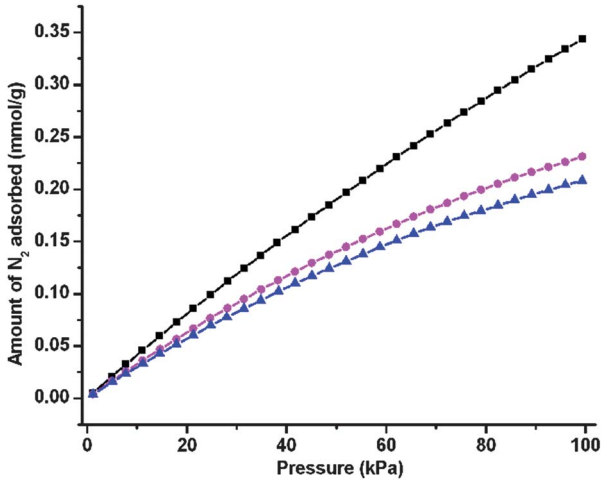

Fig. 5 Adsorption of N_2 at 273 K *versus* pressure for interpenetrated metal–organic frameworks (MOFs); black squares (■) for SUMOF-2, magenta circles (●) for SUMOF-3, and blue triangles (▲) for SUMOF-4.

As a consequence, the interaction of CO_2 with the host framework is enhanced due to its quadrupole moment. At CO_2 pressures of <40 kPa, SUMOF-3 had higher uptake than SUMOF-2 and SUMOF-4. This higher uptake means that SUMOF-3 could be a better CO_2 adsorbent for vacuum swing adsorption applications than the others. Speculatively, the enhanced low-pressure uptake of CO_2 could be related to the fact that SUMOF-3 has linkers with larger aromatic moieties than SUMOF-2 and SUMOF-4. In contrast, at pressures >90 kPa, SUMOF-3 had the lowest uptake among the three SUMOFs studied. As SUMOF-3 has a larger accessible void than the other SUMOFs, the highly curved adsorption isotherm for CO_2 indicates that SUMOF-3 would have a second step for CO_2 adsorption at higher pressures or lower temperatures than those studied. SUMOF-2 and SUMOF-4 had high uptake of CO_2 at pressures >90 kPa, which could be beneficial for gas separation processes that operate at elevated pressures.

The uptake of N_2 shows a different trend from that of CO_2. The uptake of N_2 is the largest on SUMOF-2 at all pressures studied. Its isotherm conforms to Henry's law as the uptake is linearly related to the pressure. However, for SUMOF-3 and SUMOF-4, the isotherms curve at pressures >40 kPa.

The relative uptake levels of CO_2 and N_2 could give an indication of the CO_2-over-N_2 selection in a binary mixture. By this measure it appeared that SUMOF-3 or SUMOF-4 would have higher selectivity for CO_2-over-N_2 selection at pressures relevant for a flue gas. The relative uptake of CO_2 *vis-à-vis* N_2 was 50% higher for SUMOF-3 than for SUMOF-2 at a pressure of 20 kPa.

Conclusions

Three interpenetrated MOFs (SUMOF-2, SUMOF-3 and SUMOF-4) with small pores and high specific surface areas were synthesized and characterized. Single component adsorptions of CO_2 and N_2 were determined for these materials at 273 K and various pressures. At pressures relevant for capture of CO_2 without a compression of flue gases, the uptake was greatly increased as compared to that of their non-interpenetrated counterparts. This increase can be ascribed to the enhanced interaction of CO_2 with the interpenetrated frameworks. With the aid of interpenetration in these MOFs, the electric field gradients in the small pores are increased, and therefore enhancing the interaction between CO_2 and the host framework. Still, SUMOF-2–4 showed somewhat lower uptake of CO_2 than those of aluminum-rich zeolites at such pressures of CO_2.

On the other hand, the uptake of CO_2 showed a nearly linear dependency, especially for SUMOF-2, which could be beneficial for separation of CO_2 *via* pressure swing adsorption from biogas or natural gas. For further studies of interpenetrated MOFs for a capture of CO_2 from flue gas, we believe that it would be beneficial to use linkers with heteroatoms. Such heteroatoms will further enhance the electric field gradients, and hence, the tendency to physisorb CO_2. Zn-based MOFs are very sensitive to water and a water removal step would be needed in an actual process for CO_2 capture, and we regard them as a model system. Hence, it could be important to replace the Zn_4O moiety, when developing actual sorbents.

Acknowledgements

XDZ thanks the Swedish Research Council (VR) and the Swedish Governmental Agency for Innovation Systems (VINNOVA) through the Berzelii Center EXSELENT, and the Göran-Gustafsson Foundation for nature sciences and medical research for support. NH thanks the Swedish Energy Agency for support. JS thanks the Wenner-Gren Foundations for a post-doctoral fellowship. The authors appreciate Ms Ge Liang for elemental analyses.

Notes and references

1 M. T. Ho, G. W. Allinson and D. E. Wiley, *Ind. Eng. Chem. Res.*, 2008, **47**, 4883.
2 S. Choi, J. H. Drese and C. W. Jones, *ChemSusChem*, 2009, **2**, 796.
3 N. Hedin, L. J. Chen and A. Laaksonen, *Nanoscale*, 2010, **2**, 1819–1841.
4 D. M. D'Alessandro, B. Smit and J. R. Long, *Angew. Chem., Int. Ed.*, 2010, **49**, 6058.
5 (*a*) H. K. Chae, D. Y. Siberio-Pérez, J. Kim, Y. Go, M. Eddaoudi, A. J. Matzger, M. O'Keeffe and O. M. Yaghi, *Nature*, 2004, **427**, 523; (*b*) K. Koh, A. G. Wong-Foy and A. J. Matzger, *J. Am. Chem. Soc.*, 2010, **132**, 15005; (*c*) G. Férey, C. Mellot-Draznieks, C. Serre, F. Millange, J. Dutour, S. Surblé and I. Margiolaki, *Science*, 2005, **309**, 2040; (*d*) M. Dincă and J. R. Long, *Angew. Chem., Int. Ed.*, 2008, **47**, 6766; (*e*) Y. K. Park, S. B. Choi, H. Kim, K. Kim, B.-H. Won, K. Choi, J.-S. Choi, W.-S. Ahn, N. Won, S. Kim, D. H. Jung, S.-H. Choi, G.-H. Kim, S.-S. Cha, Y. H. Jhon, J. K. Yang and J. Kim, *Angew. Chem., Int. Ed.*, 2007, **46**, 8230; (*f*) F. Song, C. Wang, J. M. Falkowski, L. Ma and W. Lin, *J. Am. Chem. Soc.*, 2010, **132**, 15390; (*g*) B. Chen, S. Xiang and G. Qian, *Acc. Chem. Res.*, 2010, **43**, 1115; (*h*) N. Klein, I. Senkovska, K. Gedrich, U. Stoeck, A. Henschel, U. Mueller and S. Kaskel, *Angew. Chem., Int. Ed.*, 2009, **48**, 9954; (*i*) P. Horcajada, C. Serre, M. Vallet-Regí, M. Sebban, F. Taulelle and G. Férey, *Angew. Chem., Int. Ed.*, 2006, **45**, 5974; (*j*) M. Xue, Y. Liu, R. M. Schaffino, S. Xiang, X. Zhao, G.-S. Zhu, S.-L. Qiu and B. Chen, *Inorg. Chem.*, 2009, **48**, 4649.
6 Y. Bae and R. Q. Snurr, *Angew. Chem., Int. Ed.*, 2011, **50**, 2.
7 B. Kesanli, Y. Cui, M. R. Smith, E. W. Bittner, B. C. Bockrath and W. Lin, *Angew. Chem., Int. Ed.*, 2004, **44**, 72.
8 M. Dincă, A. Dailly, C. Tsay and J. R. Long, *Inorg. Chem.*, 2008, **47**, 11.
9 B. Chen, S. Ma, F. Zapata, F. R. Fronczek, E. B. Lobkovsky and H. Zhou, *Inorg. Chem.*, 2007, **46**, 1233.

10 B. Chen, S. Ma, E. J. Hurtado, E. B. Lobkovsky and H. Zhou, *Inorg. Chem.*, 2007, **46**, 8490.
11 Y. E. Cheon and M. P. Suh, *Chem.–Eur. J.*, 2008, **14**, 3961.
12 L. Bastin, P. S. Bárcia, E. J. Hurtado, J. A. C. Silva, A. E. Rodrigues and B. Chen, *J. Phys. Chem. C*, 2008, **112**, 1575.
13 (*a*) G. M. Sheldrick, *Acta Crystallogr., Sect. A: Found. Crystallogr.*, 2008, **64**, 112; (*b*) A. L. Spek, *J. Appl. Crystallogr.*, 2003, **36**, 7.
14 M. Eddaoudi, J. Kim, N. Rosi, D. Vodak, M. O'Keeffe and O. M. Yaghi, *Science*, 2002, **295**, 469.
15 J. Hafizovic, M. Bjørgen, U. Olsbye, P. D. C. Dietzel, S. Bordiga, C. Prestipino, C. Lamberti and K. P. Lillerud, *J. Am. Chem. Soc.*, 2007, **129**, 3612.
16 (*a*) B. Chen, X. Wang, Q. Zhang, X. Xi, J. W. Cai, H. Qi, S. H. Shi, J. Wang, D. Yuan and M. Fang, *J. Mater. Chem.*, 2010, **20**, 3758; (*b*) G. Calleja, J. A. Botas, M. G. Orcajo and M. Sánchez-Sánchez, *J. Porous Mater.*, 2010, **17**, 91; (*c*) L. Huang, H. Wang, J. Chen, Z. Wang, J. C. Sun, D. Zhao and Y. Yan, *Microporous Mesoporous Mater.*, 2003, **58**, 105; (*d*) S. S. Kaye, A. Dailly, O. M. Yaghi and J. R. Long, *J. Am. Chem. Soc.*, 2007, **129**, 14176; (*e*) D. J. Tranchemontagne, J. R. Hunt and O. M. Yaghi, *Tetrahedron*, 2008, **64**, 8553; (*f*) H. Kim, S. Das, M. G. Kim, D. N. Dybtsev, Y. Kim and K. Kim, *Inorg. Chem.*, 2011, **50**, 3691.
17 P. L. Feng, J. J. Perry, IV, S. Nikodemski, B. W. Jacobs, S. T. Meek and M. D. Allendorf, *J. Am. Chem. Soc.*, 2010, **132**, 15487.
18 O. M. Yaghi, M. Eddaoudi, H. Li, J. Kim and N. Rosi, *US Pat.*, 6930193, **B2**, 2005.
19 (*a*) D. Y. Siberio-Pérez, A. G. Wong-Foy, O. M. Yaghi and A. J. Matzger, *Chem. Mater.*, 2007, **19**, 3681; (*b*) J. L. C. Rowsell, *Hydrogen Storage in Metal–Organic Frameworks: an Investigation of Structure–Property Relationships*, PhD dissertation, University of Michigan, Ann Arbor, MI, 2005.
20 (*a*) R. Vaidhyanathan, S. S. Iremonger, G. K. H. Shimizu, P. G. Boyd, S. Alavi and T. K. Woo, *Science*, 2010, **330**, 650; (*b*) R. Vaidhyanathan, S. S. Iremonger, K. W. Dawson and G. K. H. Shimizu, *Chem. Commun.*, 2009, 5230.
21 K. S. Walton, A. R. Millward, D. Dubbeldam, H. Frost, J. J. Low, O. M. Yaghi and R. Q. Snurr, *J. Am. Chem. Soc.*, 2008, **130**, 407.